Study of Protons in Acceptor-Doped KTaO₃ Crystals by IR and EPR Techniques

S. Q. FU, W-K LEE, AND A. S. NOWICK

*Henry Krumb School of Mines, Columbia University,
New York, New York 10027*

AND L. A. BOATNER AND M. M. ABRAHAM

*Solid State Division, Oak Ridge National Laboratory,
Oak Ridge, Tennessee 37831*

In order to understand the manner of incorporation of protons into perovskite structure oxides, KTaO₃ crystals containing acceptor dopants Co^{2+}, Mn^{2+}, Cu^{2+}, and Fe^{3+} were investigated following thermal treatments in various partial pressures of O_2 and H_2O. IR measurements were used to monitor the proton content through the OH^- absorption bands, while quantitative EPR measurements were used to determine the changes in the local environment of the dopant ion. It is shown that the introduction of protons during high-temperature treatments in H_2O is accompanied by the replacement of the oxygen-ion vacancies (V_O) that initially compensated the acceptor dopants by O^{2-} ions. In the case of the M^{2+} dopants, the dopant-vacancy association free energy is sufficiently strong to retain the $M–V_O$ pairs even during high-temperature (900°C) treatments; thus, only ⟨100⟩ axial EPR spectra due to such pairs are observed. For Fe^{3+} dopants, however, virtually all of the V_O can be replaced by O^{2-}, leaving the Fe^{3+} ion in a cubic environment. The results also show evidence for valence changes of the Co, Mn, and Cu dopants when treatments change from oxidizing to reducing atmospheres. © 1989 Academic Press, Inc.

Introduction

Although there have been many detailed studies of the defect chemistry of perovskite structure oxides such as $BaTiO_3$ and $SrTiO_3$ (*1–4*), it is only relatively recently that attention has been paid to the role of protons in materials of this type (*5, 6*). A number of authors have shown that the presence of acceptor dopants makes it possible to introduce protons readily by treatment in water vapor (*6–9*). It has been shown by means of infrared (IR) absorption measurements, that an interstitial proton combines with an adjacent O^{2-} ion to form an OH^- center; thus the IR absorption due to OH^- provides the most direct evidence for the presence of protons in the lattice. Of particular interest is the possibility of obtaining protonic conductors from such materials. In fact, Iwahara *et al.* (*8*) have shown that ceramic samples of acceptor-doped $SrCeO_3$ and $BaCeO_3$ treated in water vapor are indeed good protonic conductors,

while Lee *et al.* (*9, 10*) showed that single crystals of $KTaO_3$ doped with transition-metal ions conduct primarily by proton hopping.

In view of these results, it is desirable to determine the nature of the reaction by which protons are introduced into the acceptor-doped crystal through a high-temperature treatment in water vapor. Two reactions that can be enhanced by acceptor dopants may be considered, as follows (using Kröger–Vink notation):

$$H_2O(g) + V_O^{\cdot\cdot} \rightarrow 2H_i^{\cdot} + O_O^x \qquad (1)$$

$$H_2O(g) \rightarrow 2H_i^{\cdot} + \tfrac{1}{2}O_2(g) + 2e'. \qquad (2)$$
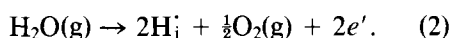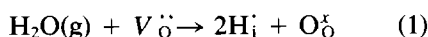
(Throughout this paper we will regard $H_i^{\cdot}$ and $OH_O^{\cdot}$ as equivalent.) The first reaction has been the most widely suggested. Since an acceptor dopant M is a lower valent cation substituting on the B-site of the ABO_3 perovskite, it can be described as M_B' or M_B'' (depending on the difference in charge state of cations M and B). The most likely defect to charge compensate such acceptor dopants is the oxygen vacancy $V_O^{\cdot\cdot}$ (*11*), which thus provides the basis for reaction (1). On the other hand, reaction (2) might be favored if the acceptor dopant has multiple valency, so that it can absorb the electrons produced by this reaction, for example, by M^{3+} ions becoming M^{2+}.

Potassium tantalate, $KTaO_3$, is an ideal perovskite oxide for the study of such processes since it has the cubic structure at all temperatures between 1 K and its melting point (1630 K) and does not undergo a ferroelectric or other phase transformation of the type that makes the study of either $BaTiO_3$ or $SrTiO_3$ more complex. Also, it has been shown that various transition-metal ions can be readily incorporated in single crystals of $KTaO_3$ where they substitute for Ta (*12*). Finally, the electron paramagnetic resonance (EPR) spectra of these transition-metal acceptor dopants in $KTaO_3$ have been previously investigated,

and these results provide useful information regarding the local environment of the impurity ion (*12–18*). Specifically, a $\langle 100 \rangle$ axial spectrum, attributed to nearest-neighbor M–V_O pairs, has been observed for each of the transition-metal ion dopants.

The present work builds on these previous studies of transition-metal-doped $KTaO_3$ crystals by combining IR measurements (to monitor the OH^- content) with quantitative EPR studies, in order to follow the changes in the defect structure of the dopant ion that result from thermal treatments in different oxygen or water-vapor partial pressures, $P(O_2)$ and $P(H_2O)$, respectively. The goal of this investigation is to increase our understanding of the defect chemistry of the dopant ions as well as the mechanisms by which protons are incorporated into the perovskite lattice.

Experimental Methods

Single crystals of $KTaO_3$ were grown by a technique similar to that described previously by Hannon (*19*). The acceptor dopants (Co^{2+}, Mn^{2+}, Cu^{2+}, or Fe^{3+}) were added to the melt in amounts of 0.1 to 1.0 mol%; however, crystals that were chemically analyzed showed smaller dopant concentrations, ranging from 0.01 to 0.1 mol%. Samples cut from the as-grown crystals were treated at 900°C in different atmospheres including O_2, 1% O_2, Ar, and CO/CO_2 (a 50/50 mixture for which $P(O_2) = 10^{-16}$ atm). These gases were used either "dry" (i.e., passed through a liquid nitrogen trap) or "wet" (i.e., bubbled through water at room temperature). In addition some samples were treated in a mechanically pumped vacuum ($\sim$40 mTorr). The treatment time in all cases was between 6 and 8 hr.

The IR measurements were made at room temperature in a Perkin–Elmer Model 1800 Fourier transform infrared spectrophotometer.

The details of the electron paramagnetic resonance (EPR) measurements are described elsewhere (12). The frequency employed is 9.2 GHz and the range of the magnetic field is from 0 to 12 kG. The measurements on Co^{2+} were carried out at liquid helium temperatures, while the other measurements were done at 85 K and at room temperature. EPR spectra were observed only for Co^{2+}, Mn^{2+}, Cu^{2+}, and Fe^{3+}, so that changes in valence of these ions had to be inferred from changes in the spectral intensities.

Results

IR Measurements

Room-temperature infrared measurements were carried out on KTaO₃ samples each containing one of the dopants: Co, Mn, Cu, or Fe. In all cases, the main OH^- absorption peak observed was at 3473 cm^{-1} with a half-width of 5.7 cm^{-1}, independent of the dopant. In addition, a secondary peak was observed at 3480 cm^{-1} for the Cu, Mn, and Fe-doped samples with a peak height of only 10 to 20% of that of the main peak. For the Co dopant, the secondary peak was either absent or very weak. These results are consistent with those reported previously on nominally pure samples (7).

Table I lists the IR intensities of the main OH^- peak for various samples treated at

TABLE I

IR ABSORPTION, α_{OH}(IN cm^{-1}), AT THE MAIN PEAK, 3473 cm^{-1} FOR VARIOUSLY DOPED KTaO₃ CRYSTALS

Atmosphere	Co-a	Mn	Cu	Fe-a	Fe-b
CO/CO₂	4.53	7.42	3.58	3.25	0.85
Ar	4.23	7.21	3.15	3.18	—
O₂	4.12	5.89	3.05	3.09	0.81

Note. All samples were pretreated at 900°C in water-saturated gases. (The designation -a and -b refer to samples from different growths.)

TABLE II

IR ABSORPTION AT 3473 cm^{-1} OF A CO-DOPED SAMPLE (Co-b) FOLLOWING TREATMENT IN DIFFERENT $P(H_2O)$

Treatment	$P(H_2O)$ (atm)	α_{OH} (cm^{-1})
Vacuum	~10^{-6}	0.2
Dry Air	~10^{-4}	0.5
Undried air	2×10^{-2}	2.5
Ar + H₂O	3×10^{-2}	2.7
Steam	1	2.7

900°C in O₂, Ar, or CO/CO₂ gases, all of which were saturated with water vapor at room temperature. The quantity α_{OH} in the table is the absorption coefficient of the main OH^- peak. It is noteworthy that α_{OH} is always somewhat higher for reducing atmospheres than it is for oxidizing conditions, with the ratio varying from 1.26 for Mn doping to only 1.05 for Fe doping. (The two Fe-doped samples studied came from different crystals.) The secondary OH^- peaks generally follow a similar pattern.

The effects of a wider range of treatments in various atmospheres, including dry gases and vacuum, are shown in Table II for a Co-doped sample. Two important conclusions may be drawn from these results that are valid for the other dopants as well. The first conclusion is that the saturation of α_{OH} occurs at a water vapor partial pressure, $P(H_2O)$, of approximately 10^{-2} atm. Gases saturated with water at room temperature (such as reported in Table I) fall within this saturation range. Second, despite our efforts to dry the gases carefully, the lowest α_{OH} values were obtained for vacuum-treated samples and typically fell in the range from 0.2 to 0.3 cm^{-1}, while for dry gases the values were somewhat higher, i.e., ~0.4 cm^{-1}.

EPR Measurements

As previously noted, the EPR spectrum for each of the four dopants was observed only for a single valence state, i.e., Co^{2+},

FU ET AL.

Mn^{2+}, Cu^{2+}, and Fe^{3+}. Despite this limitation, the relative EPR spectral intensities can be used to infer whether or not changes in the oxidation state of the dopant ions take place as a consequence of thermal treatments in various atmospheres. Significant differences exist between the EPR spectra of Co, Mn, and Cu-doped crystals and that of Fe-doped samples; accordingly, the results for these two cases will be presented separately.

The most striking feature of the EPR spectra for the divalent ions Co^{2+}, Mn^{2+}, and Cu^{2+} is that in each case, regardless of the thermal treatment, only a single axial spectrum is observed. These spectra have been previously reported (12–16) and, in each case, they exhibit $\langle 100 \rangle$ axial symmetry. Only the relative intensity of the spectra changes with thermal treatment. These intensity variations are summarized in Table III, where the relative intensities under reducing (CO/CO_2) conditions are compared with those under oxidizing (either 1% O_2 or pure O_2) conditions with the gases either dry or water-saturated (wet). In all cases there is no significant change for the wet vs dry spectra for the same $P(O_2)$, except possibly in the case of Co^{2+} in wet and dry CO/CO_2 where a small difference that appears to be outside of experimental error is observed. On the other hand, large

TABLE III

EPR Measurements of the Co^{2+} [Sample Co-a], Mn^{2+}, AND Cu^{2+} Axial Spectra in Doped $KTaO_3$ Crystals Following Different Thermal Treatments

Treatment	Co^{2+}	Mn^{2+}	Cu^{2+}
Wet CO/CO_2	8	1.9	1
Dry CO/CO_2	6	1.8	1
Wet 1% O_2	1	—	15
Dry 1% O_2	1	—	15
Wet O_2	—	1.1	—
Dry O_2	—	1.0	—

Note. Intensities in arbitrary units.

TABLE IV

Intensities of Axial and Cubic EPR Spectra of Fe^{3+} (I_{ax} AND I_{cub}, Respectively) and Total Fe^{3+} in Axial Units[a]

Treatment	I_{ax}	I_{cub}	Total Fe^{3+}
Wet CO/CO_2	1.0	2.3	15.5
Dry CO/CO_2	9.0	1.0	15.3
Wet O_2	1.2	2.5	17.0
Dry O_2	5.0	1.9	17.0
Vacuum	12.4	0	>12.4

[a] Taking 6.3 I_{cub} + I_{ax} = total Fe^{3+}. (Results are for sample Fe-b.)

changes in intensity with changes in $P(O_2)$ are found. In particular, the Co^{2+} and Mn^{2+} spectra are significantly stronger after treatment in a reducing atmosphere, while the Cu^{2+} spectrum is much stronger after treatment in an oxidizing environment. These results are consistent with the expected valence changes of Co^{2+} going to Co^{3+} and Mn^{2+} going either to Mn^{3+} or Mn^{4+} when oxidized, and with Cu^{2+} changing to Cu^+ in a reducing atmosphere.

The observed valence changes with changing $P(O_2)$ are not surprising. The most significant result for these three dopants, however, is the failure to observe a cubic spectrum following any of the treatments employed and the essentially unchanged intensities following the wet and dry thermal anneals. This latter result must be regarded as excluding reaction (2) for these dopants.

In the case of Fe-doped $KTaO_3$ samples, quite different results are obtained. First, as previously reported (18), two Fe^{3+} EPR spectra are obtained, viz., a cubic and a $\langle 100 \rangle$ axial spectrum, and appreciable changes occur in the relative intensities of the spectra for the wet and dry pretreatments. Table IV presents the results for the sample designated in Table I as Fe-b. The intensity of the axial and cubic spectra, denoted as I_{ax} and I_{cub}, respectively, are listed in arbitrary units for a variety of wet

and dry thermal treatments. It is clear that, under both oxidizing and reducing conditions, I_{ax} is higher for dry than for wet atmospheres, while the reverse is true for I_{cub}. These results are similar to those reported earlier by Gonzalez *et al.* (*18*). If it is further assumed that, in going from dry to wet for a given $P(O_2)$, one spectrum is being "exchanged" for the other, it is readily obtained from the data both for CO/CO_2 and O_2 atmoshperes that $\delta I_{ax}/\delta I_{cub}$ = −6.3. (Here δI_{ax} and δI_{cub} are the changes in the two spectra in the arbitrary units used.) Accordingly, it is concluded that the conversion factor of 6.3 may be used to change the arbitrary units of I_{cub} into units of I_{ax}. On this basis, the final column of Table IV gives the total Fe^{3+} content in axial units. The total Fe^{3+} in the reduced case is then 15.3–15.5 while that for the oxidized case is 17.0. This is consistent with the conversion of about 10% of the Fe^{3+} to Fe^{2+} under reducing conditions, which is a considerably less drastic change than the degree of the oxidation–reduction reaction that occurs for Co, Mn, and Cu.

The results for vacuum treatment of the Fe-doped sample are most striking. The axial spectrum increases in intensity while the cubic spectrum disappears completely. In addition, at least two new low-symmetry spectra are observed which have not been previously reported. Figure 1 shows the comparison between the usual axial-plus-cubic spectra for a sample treated in a wet gas with that obtained after vacuum treatment. The new Fe^{3+} spectra are characterized as follows:

(a) the symmetry is low, perhaps lower than uniaxial;

(b) the crystal field splitting is relatively large, and the magnitudes are sensitive to temperature;

(c) all of the EPR lines absorb power strongly, i.e., they do not saturate easily, and some show superhyperfine structure.

In view of the unusual nature of these results, a vacuum treatment was also carried out on a sample from another Fe-doped crystal (Fe-a) with similar results. In contrast, vacuum treatments of samples containing each of the other dopants did not produce similar low-symmetry spectra.

From the value of I_{ax} given in the last row of Table IV, it is clear that the vacuum treatment produces two changes relative to a dry gas treatment. First, some additional cubic spectrum is converted to axial; this is consistent with the further lowering of α_{OH} under vacuum. Second, the remaining cubic spectrum appears to have been converted to the new low-symmetry spectra. An attempt to identify these new spectra by observing their angular variation is difficult due to several factors, such as the profusion and low intensity of the lines and the high dielectric constant of $KTaO_3$. Clearly, a determination of the precise nature of the Fe defect that gives rise to these new spectra will require further detailed study.

Discussion

The feature common to all four paramagnetic dopants in $KTaO_3$ is that in each case they display a ⟨100⟩ axial EPR spectrum that has been attributed to the nearest-neighbor M–V_O pair. This interpretation of the axial spectra seems to be firmly established and, therefore, forms the basis for the following discussion.

Considering first the case of Fe-doped crystals, it is clear that the Fe^{3+} spectrum changes from axial to cubic as a result of thermal treatment in water vapor. A cubic-to-axial conversion ratio has been found (Table IV), and this result is clearly consistent with reaction (1) in which vacancies, $V_O^{\cdot\cdot}$, are replaced by oxygen ions and thus leave the Fe^{3+} ions in a cubic environment. The presence of residual cubic Fe^{3+} in samples treated in dry gases may be related to the observation of residual OH^- in such
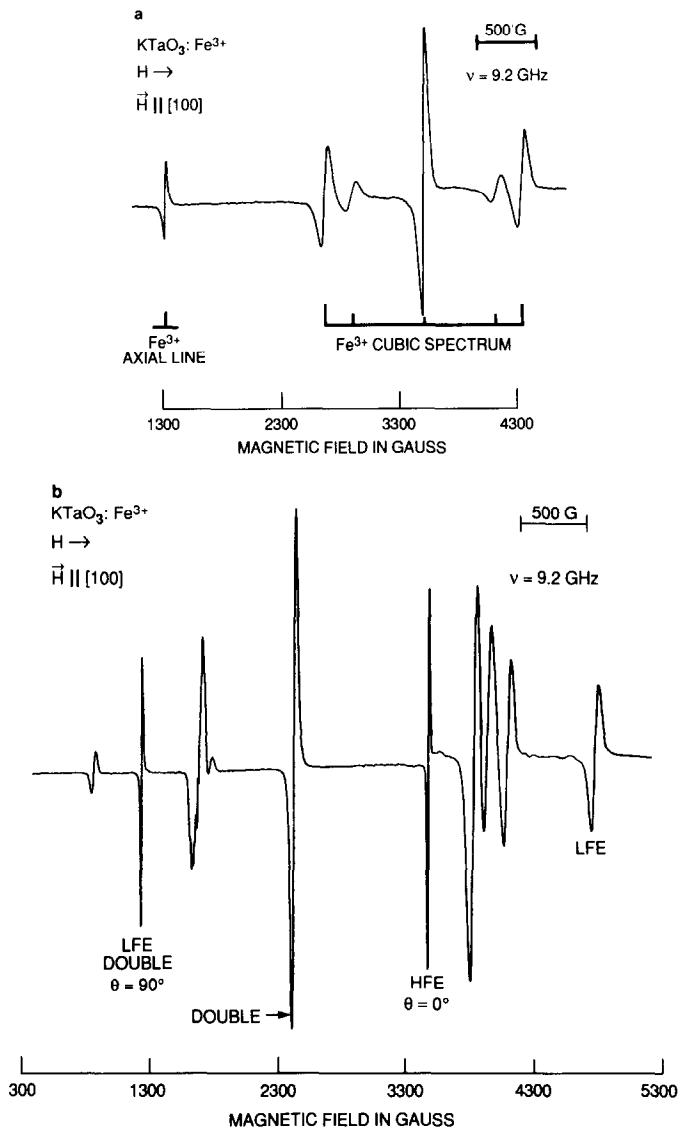
FIG. 1. EPR spectra of Fe^{3+}-doped $KTaO_3$ for field parallel to [100]: (a) following treatment in water vapor; (b) following vacuum treatment. LFE and HFE refer to low- and high-field extremals, respectively. "Double" means that two lines fall together at this orientation.

samples (usually such that $\alpha_{OH} \sim 0.4\ cm^{-1}$). The effect of $P(O_2)$ on the Fe-doped samples is relatively small (Table IV) and suggests that Fe remains primarily in the 3+ valence state even in the most reducing atmosphere employed.

As already mentioned, the effect of vac- uum treatment is to convert some of the residual cubic spectrum to axial and to convert the remaining cubic to the new low-symmetry spectra. At present, it is not clear why this change occurs. The observed changes in the spectra cannot be due to the lowered $P(O_2)$ under vacuum, since under

the CO/CO_2 treatment the value of $P(O_2)$ is many order of magnitude lower but still the new spectra do not appear. Further investigation will be required to account for the new Fe^{3+} spectra which appear as a result of treatment under vacuum.

The most important conclusion in the case of Fe dopants is that reaction (1) can explain the principal facts. When oxygen vacancies are the compensators for the acceptor dopants they associate with the Fe^{3+} ions at the lower temperatures to produce $\langle 100 \rangle$ axial defect pairs; upon reaction with water, the vacancies are replaced by oxygen ions leaving Fe^{3+} ions in a cubic environment, while the charge-compensating protons are well separated from the Fe^{3+} ions.

Turning now to considerations of the three divalent dopants Co, Mn, and Cu, it is anticipated that, in the absence of protons, compensation will take the form:

$$M'''_{Ta} + (\tfrac{3}{2})V_O^{\cdot\cdot}$$
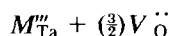
i.e., an additional half-vacany per dopant ion is required compared to the case of Fe^{3+}. EPR analysis, however, shows only the $\langle 100 \rangle$ axial spectra that are interpreted as due to $M-V_O$ pairs. The striking effects of various $P(O_2)$ treatments (see Table III) are consistent with the expected valence changes: Co^{2+} and Mn^{2+} being strongest after treatment in a reducing atmosphere, while Cu^{2+} is strongest following heating in an oxidizing atmosphere. The absence of any significant change in intensity following water treatments appears to eliminate reaction (2) as playing a major role in the introduction of protons and, therefore, takes us back to reaction (1) in this case as well. It is, somewhat surprising, however, that cubic spectra are not observed after treatments in water vapor. It appears, therefore, that reaction (1) takes place only to the extent of replacing the extra half-vacancy by oxygen. If the $M-V_O$ pairs were fully dissociated at the treatment tempera-

ture of 900°C, this would suggest that no more than one-third of the available oxygen vacancies are replaced in the reaction. Such a result, however, is inconsistent with the observation that, under normal $P(H_2O)$, the reaction goes essentially to saturation (see Table II). Accordingly, we must consider the alternative of a strong $M-V_O$ association even at 900°C, so that only the free extra half-vacancy is replaced by oxygen while the $M-V_O$ pair remains intact. The association reaction is

$$M'''_{Ta} + V_O^{\cdot\cdot} \rightleftharpoons P', \qquad (3)$$
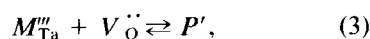
where P' denotes the pair, $M-V_O$, that carries an effective negative charge. The mass-action equation for this association reaction is

$$c_M c_V / c_P = K_A = (\tfrac{1}{6}) \exp(-G_A/kT), \quad (4)$$

where c_M, c_V, and c_P are the concentrations (mole fractions) of M_{Ta}, V_O, and pairs, respectively, while G_A is the free energy of association and the factor $\tfrac{1}{6}$ comes from the six equivalent orientation of the pair. In addition to Eq. (4) we require the mass-action equation for reaction (1),

$$c_H^2 / c_V = K_w P(H_2O), \qquad (5)$$

where c_H is the mole fraction of interstitial protons. To these we add the dopant conservation equation

$$c_M + c_P = c_t, \qquad (6)$$

where c_t is the total dopant concentration, and the charge conservation equation

$$2c_V + c_H = 3c_M + c_P. \qquad (7)$$

We seek a solution for the case in which there is no detectable cubic spectrum, so that

$$10\, c_M < c_P \simeq c_t, \qquad (8)$$

where the last step utilizes Eq. (6). Further, we require that reaction (1) proceed close to saturation, meaning that the free V_O are almost fully replaced by oxygen while the

M–V_O pairs remain intact. For this to occur, we must have $c_H \sim c_t$ while c_V is small compared to c_H, which may reasonably be accomplished by taking $10c_V < c_t$. Putting this result and Eq. (8) into Eq. (4) then gives $K_A < 10^{-2} c_t$. Utilizing the expression for K_A in Eq. (4) and a typical value for c_t of $\sim 3 \times 10^{-4}$ and a temperature of 900°C, we obtain $G_A > 1.10$ eV. Such a large value for the free energy of association is not unreasonable considering the large coulombic interaction that exists between M''' and $V_O^{\cdot\cdot}$.

For the M ion oxidized to a 3+ state (i.e., M''_{Ta}), Eqs. (4)–(6) are still valid, but Eq. (7) becomes

$$2c_V + c_H = 2c_M \qquad (9)$$

since the pairs are now neutral. Under these conditions, the coulombic interaction that binds the pair falls to $\frac{2}{3}$ of the value for the case in which M is in the 2+ state. Thus, for example, G_A may fall from 1.1 to 0.73 eV. Such a change increases K_A by a factor of about 40, enough to lead to a solution of these equations in which the pairs are substantially dissociated at 900°C, i.e., with $c_M \sim c_P$. In this case, an appreciable fraction of M^{3+} dopants should be present in a cubic environment following the treatment, but due to the fact that the EPR measurements on Co, Mn, and Cu observe the paramagnetic ion only in the 2+ state, we are unable to observe such a cubic spectrum directly.

These considerations lead to the conclusion (for example for the case of Co doping) that, despite the higher concentration of oxygen vacancies after treatment in a reducing atmosphere, α_{OH} should be lower than after treatment in an oxidizing atmosphere. Such a conclusion, however, is at variance with the results of Table I. The observed IR results can be accounted for, however, if, unlike the case of Fe^{3+}, the solution of Eqs. (4)–(6) and (9) for the case of Co^{3+} dopants involves an equilibrium in which both Co–V_O pairs and isolated Co''_{Ta}

are present in appreciable fractions. This can occur if G_A is slightly larger for Co–V_O than for Fe–V_O pairs, thus favoring partial association at 900°C for the case of Co. The situations for Mn and for Cu are more complicated because of the occurrence of Mn^{4+} and of Cu^+.

Conclusions

Oxygen ions and protons are introduced during high-temperature H_2O treatments, with the O^{2-} replacing $V_O^{\cdot\cdot}$ defects and protons occupying interstitial sites and providing charge compensation for acceptor dopants [reaction (1)]. For Fe^{3+} dopants, most of the vacancies are replaced in this way, leaving Fe^{3+} ions in a cubic environment. In the case of M^{2+} dopants (Co^{2+}, Mn^{2+}, and Cu^{2+}), however, the association free energy G_A is so strong as to allow only $\frac{1}{2}$ V_O per dopant to be replaced by oxygen during the treatment, so that exclusively M–V_O $\langle 100 \rangle$ axial spectra are still observed after oxygen and protons are introduced.

The effects of oxidizing and reducing treatments are also observed, showing substantial conversions of Co^{2+} into Co^{3+} and of Mn^{2+} into Mn^{3+} or Mn^{4+} under oxidizing atmospheres, and of Cu^{2+} into Cu^+ under reducing atmospheres. The valence changes of Fe are much smaller, and Fe remains primarily in the 3+ state.

Acknowledgments

References

1. L. C. WALTER AND R. E. GRACE, J. Phys. Chem. Solids 28, 239 (1967).

2. M. E. LINES AND A. M. GLASS, "Principles and Application of Ferroelectrics and Related Materials," Clarendon Press, Oxford (1977).

3. D. M. SMYTH, *Prog. Solid State Chem.* **15**, 145 (1984).

4. D. M. SMYTH, *Annu. Rev. Mater. Sci.* **15**, 329 (1985).

5. S. KAPPHAN, J. KOPPITZ, AND G. WEBER, *Ferroelectrics* **25**, 585 (1980); **37**, 673 (1981).

6. R. WASER, *J. Amer. Ceram. Soc.* **71**, 58 (1988).

7. H. ENGSTROM, J. B. BATES, AND L. A. BOATNER, *J. Chem. Phys.* **73**, 1073 (1980).

8. H. IWAHARA, T. ESAKA, H. UCHIDA, AND N. MAEDA, *Solid State Ionics* **3/4**, 359 (1981); **11**, 109 (1983).

9. W-K LEE, A. S. NOWICK, AND L. A. BOATNER, *Adv. Ceram.* **23**, 387 (1987).

10. W-K LEE, A. S. NOWICK, AND L. A. BOATNER, *Solid State Ionics* **18/19**, 989 (1986).

11. G. V. LEWIS, AND C. R. A. CATLOW, *J. Phys. Chem. Solids* **47**, 89 (1986).

12. M. M. ABRAHAM, L. A. BOATNER, D. N. OLSON AND U. T. HÖCHLI, *J. Chem. Phys.* **81**, 2528 (1984).

13. D. M. HANNON, *Phys. Rev.* **164**, 366 (1967); **B3**, 2153 (1971).

14. D. M. HANNON, *Phys. Status Solidi B* **43**, K21 (1971).

15. L. A. BOATNER, A. H. KAYAL, AND U. T. HÖCHLI, *Helv. Phys. Acta* **50**, 167 (1977).

16. I. N. GEIFMAN, *Phys. Status Solidi B* **85**, K5 (1978).

17. K. A. MÜLLER, *J. Physique* **42**, 551 (1981).

18. R. GONZALEZ, M. M. ABRAHAM, L. A. BOATNER, AND Y. CHEN, *J. Chem. Phys.* **78**, 660 (1983).

19. D. M. HANNON, Scientific Report No. 7, AFCRL-66-303, Air Force Cambridge Research Laboratory, Bedford, MA (1966).